nature structural & molecular biology

Inhibition of CED-3 zymogen activation and apoptosis in *Caenorhabditis elegans* by caspase homolog CSP-3

Xin Geng[1], Yong Shi[1], Akihisa Nakagawa[1], Sawako Yoshina[2], Shohei Mitani[2], Yigong Shi[3] & Ding Xue[1]

Inhibitor of apoptosis (IAP) proteins have a crucial role in apoptosis, through negative regulation of caspases in species from fruitflies to mammals. In *Caenorhabditis elegans*, however, no IAP homolog or caspase inhibitor has been identified, calling into question how the cell-killing caspase CED-3 can be negatively regulated. Here we show that inactivation of the *C. elegans csp-3* gene, which encodes a protein similar to the small subunit of the CED-3 caspase, causes cells that normally live to undergo apoptosis in a CED-3–dependent manner. Biochemical analysis reveals that CSP-3 associates with the large subunit of the CED-3 zymogen and inhibits zymogen autoactivation. However, CSP-3 does not block CED-3 activation induced by CED-4, nor does it inhibit the activity of the activated CED-3 protease. Therefore CSP-3 uses a previously unreported mechanism to protect cells from apoptosis.

© 2008 Nature Publishing Group http://www.nature.com/nsmb

Programmed cell death (apoptosis) is a fundamental process in the development and tissue homeostasis of metazoans[1]. During apoptosis, a suicide machinery is activated to dismantle the cell[1]. An essential component of the apoptotic machinery is the caspase, a family of cysteine proteases that execute apoptosis by cleaving specific cellular protein substrates after aspartate residues[2]. All caspases are initially synthesized as latent zymogens, each comprising an N-terminal prodomain and two catalytic subunits known as the large and the small subunits[2]. The activation of the caspase zymogens proceeds by autoproteolysis through induced dimerization or oligomerization of the caspase zymogens, or through proteolytic cleavage by upstream caspases or cysteine proteases[3,4]. Once activated, caspases cleave a broad spectrum of cellular targets, leading to the demise of the cell.

Given the crucial roles of caspases in apoptosis, it is imperative that their activities be tightly regulated. The control of caspase activity can be achieved at two different levels—the activation of caspase zymogens and the catalytic activity of activated caspases—and by both positive and negative regulators[5]. As caspases are widely expressed in many cells[6], elaborate mechanisms must be in place to prevent inadvertent activation of caspases in cells that normally live. In cells that receive apoptotic stimuli or cells that are destined to die, positive regulators are unleashed to promote the activation of caspase zymogens. One such positive regulator is mammalian apoptotic protease activating factor-1 (Apaf1), which activates the caspase-9 zymogen through formation of an oligomeric apoptosome upon the release of cytochrome *c* from mitochondria[7–9]. In *Caenorhabditis elegans*, the Apaf1 homolog CED-4 activates the CED-3 zymogen through a similar oligomerization event, after the cell-death initiator EGL-1 binds to the cell-death inhibitor CED-9 and triggers the dissociation of the CED-4 dimer from CED-9 tethered on the surface of mitochondria[10–14]. These observations suggest that the general mechanisms of caspase activation are conserved from *C. elegans* to mammals, although the details may vary in different organisms[3,4].

To prevent inadvertent cell death, various negative regulators of apoptosis are used by cells to keep the apoptotic machinery in check. For example, the Bcl-2 family of cell-death inhibitors and their worm homolog CED-9 prevent Apaf1 and CED-4 from forming oligomeric apoptosomes in mammals and *C. elegans*, respectively[9,15]. The IAPs, characterized by at least one baculoviral IAP repeat (BIR) and a RING-finger motif[16], are dedicated negative regulators of caspases in *Drosophila melanogster* and higher organisms[17–21]. IAP proteins have been shown to inhibit directly the activation of caspase zymogens and the catalytic activity of activated caspases[16,22–24]. Intriguingly, no IAP homolog or caspase inhibitor has been identified in *C. elegans*, whereas other key components of apoptosis were found to be highly conserved[25], raising the important question of how the activation and the activity of the CED-3 caspase are regulated in *C. elegans*. Here, we show that the product of the *csp-3* gene, a protein similar to the small subunit of CED-3, functions as a direct caspase inhibitor to prevent cells that normally live from undergoing apoptosis.

RESULTS

Loss of *csp-3* causes increased cell deaths

csp-3 is one of the three additional caspase-like genes in *C. elegans* that have no known functions[26]. Unlike regular caspases, CSP-3 does not contain a caspase large subunit with a cysteine in its active site and is

[1]Department of Molecular, Cellular, and Developmental Biology, Campus Box 347, University of Colorado, Boulder, Colorado 80309, USA. [2]Department of Physiology, Tokyo Women's Medical University, School of Medicine, and Core Research for Evolutional Science and Technology, Japan Science and Technology Agency, 8-1, Kawada-cho, Shinjuku-ku, Tokyo, 162-8666, Japan. [3]Department of Molecular Biology, Washington Road, Princeton University, Princeton, New Jersey 08544, USA. Correspondence should be addressed to D.X. (ding.xue@colorado.edu).

Received 9 June; accepted 5 August; published online 7 September 2008; doi:10.1038/nsmb.1488

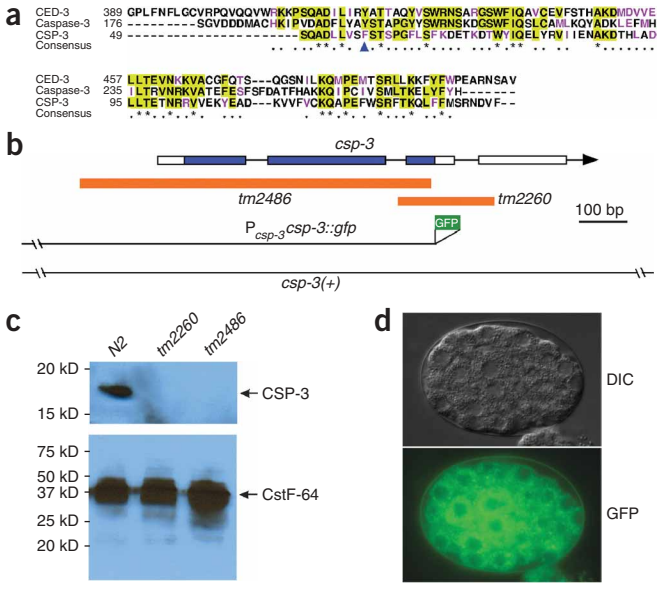

Figure 1 CSP-3 is a cytoplasmic protein with sequence homology to the small subunit of CED-3. (**a**) Sequence alignment of CSP-3 and the small subunits of CED-3 and human caspase-3. Residues that are identical are shaded in yellow and residues that are similar are labeled with pink. Phe57 of CSP-3 is indicated with a blue arrowhead. (**b**) The *csp-3* gene structure and deletion mutations. Exons are depicted as boxes and introns as lines. The translated regions of *csp-3* are highlighted in blue. Two orange boxes indicate the regions of *csp-3* removed by the two *csp-3* deletions, respectively. Also shown are a *csp-3* translational *gfp* fusion and a 5.73-kb genomic rescuing fragment (*csp-3*(+)). (**c**) Both *csp-3* deletions abolish expression of *csp-3* in *C. elegans*. Immunoblotting for CSP-3 in total worm lysates from *N2, csp-3*(*tm2260*) and *csp-3*(*tm2486*) animals is shown. The CstF-64 protein was used as a loading control. (**d**) *csp-3* is ubiquitously expressed in *C. elegans* embryos. Differential interference contrast (DIC) and GFP images of an early-stage embryo carrying $P_{csp\text{-}3}$*csp-3::gfp* are shown.

predicted to lack proteolytic activity (**Fig. 1**). Its sequence similarity to the small subunits of caspases (**Fig. 1a**) and the fact that the small and the large subunits of caspases form heterotetramers during caspase activation suggest that CSP-3 may associate with other caspases such as CED-3 and modulate the activation of CED-3. To investigate the function of *csp-3* in *C. elegans*, we generated two deletion alleles of *csp-3*: *tm2260* and *tm2486*. In *tm2260*, a 193-base-pair (bp) region of the *csp-3* gene is removed, including the last exon and part of the 3′ untranslated region (UTR). *tm2486* contains a 713-bp deletion that almost removes the entire coding region of *csp-3* (**Fig. 1b**). Both deletions abolished the expression of *csp-3* in *C. elegans* and are putative null alleles (**Fig. 1c**).

We first examined whether cell death occurred normally in *csp-3*(*tm2486*) and *csp-3*(*tm2260*) mutants by counting cells present in the anterior pharynx of these animals. Among 29 cells that normally live (**Supplementary Table 1** online), approximately 40% of *csp-3* mutant animals were missing one or two cells, whereas cells that normally die were unaffected. To investigate the cause of missing cells in *csp-3* mutants, we counted the number of apoptotic cell corpses in various embryonic stages and found that *csp-3*(*tm2486*) and *csp-3*(*tm2260*) animals had slightly higher numbers of apoptotic cells in some embryonic stages than wild-type animals (**Fig. 2a**). Because apoptotic cells are swiftly engulfed in *C. elegans* by their neighboring cells, this assay would not detect a small increase in apoptosis. We thus constructed double mutants containing a *csp-3* mutation and a mutation that partially disables cell-corpse engulfment such as *ced-5*(*n1812*) or *ced-6*(*n2095*)[27]. The *csp-3*;*ced-5* and *csp-3*;*ced-6* double mutants had substantially more cell corpses in most embryonic stages and in the L1 larval stage than *ced-5*, *ced-6* or *csp-3* single mutants (**Fig. 2b**,**c**). The increased numbers of cell corpses in *csp-3*;*ced-5* and *csp-3*;*ced-6* double mutants indicate that *csp-3* mutations either result in increased cell deaths or compromise cell-corpse engulfment. As cells that normally live were missing in the *csp-3* mutants (**Supplementary Table 1**), these results are more consistent with *csp-3* mutations causing ectopic cell deaths.

The phenotype of increased numbers of cell corpses in *csp-3* (*tm2260*);*ced-5*(*n1812*) animals could be rescued through germline transformation by a 5.73-kb genomic fragment containing the *csp-3*-coding region flanked by 4,149-bp promoter and a 1,017-bp 3′ UTR region (**Figs. 1b** and **2d**). We could also rescue the *csp-3* mutants by ubiquitously expressing *csp-3* under the control of the *dpy-30* gene promoter ($P_{dyp\text{-}30}$*csp-3*) or the *sur-5* gene promoter ($P_{sur\text{-}5}$*csp-3*)[28,29] (**Fig. 2d**), suggesting that loss of the *csp-3* activity causes increased apoptosis. The $P_{sur\text{-}5}$*csp-3* transgene, which caused widespread overexpression of *csp-3* in *C. elegans* (**Fig. 2e**), only mildly inhibited normal programmed cell death in wild-type animals (**Fig. 2f**). In addition, loss of *csp-3* did not reduce the number of cells that escape apoptotic cell fates in the anterior pharynx of *ced-3(n2438)* animals, which is partially defective in cell death, but still caused loss of normal cells, albeit at a reduced frequency (**Supplementary Table 1**). These observations suggest that *csp-3* protects cells that normally live but does not seem to affect cells that are destined to die.

csp-3 protects cells that normally live from apoptosis

We further characterized the missing cell phenotype of the *csp-3* mutants using various integrated transgenes carrying GFP reporters that label different cells or cell types and thus allow clear identification of the cells that are lost in the *csp-3* mutants. For example, the $P_{mec\text{-}4}$*gfp* construct in the *bzIs8* transgene specifically labels six touch-receptor neurons[30]. In *csp-3*(*lf*); *bzIs8* animals, all six touch cells were randomly lost (at a frequency from 2% to 10%; **Fig. 3a**) and 30–34% of animals lost at least one touch cell (data not shown). The dying touch cells in the *csp-3* mutants had a raised button–like morphology characteristic of apoptotic cells (**Fig. 3b**). The missing cell defect in *csp-3* mutants was rescued by the 5.73-kb *csp-3*(+) transgene (**Fig. 3c**) and was strongly suppressed by loss-of-function mutations in the *egl-1*, *ced-4* and *ced-3* genes (**Fig. 3a**), all of which are essential for *C. elegans* programmed cell death[25]. A similar percentage of animals (37–39%) randomly lost at least one neuron in *csp-3*(*lf*);*inIs179* animals, in which different sets of neurons including the phasmid neurons (PHA, PHB and PHC), ventral cord neurons (VC), hermaphrodite-specific neurons (HSN) and ADE neurons were labeled by the $P_{ida\text{-}1}$*gfp* reporter present in the *inIs179* transgene[31] (**Fig. 3d**). Again, such cell loss was strongly suppressed by a loss-of-function mutation (*n2433*) in the *ced-3* gene (**Fig. 3d**). As the missing neurons are cells that normally live, these results confirm that *csp-3* has an important role in protecting cells that normally live from apoptosis.

Loss of *csp-3* causes low-percentage embryonic lethality

We also examined whether random loss of living cells in *csp-3* mutants might result in developmental abnormalities, such as those seen in animals defective in another antiapoptosis gene, *ced-9* (ref. 32). We found that 5–6% of *csp-3* mutant embryos failed to hatch, and approximately 2% of *csp-3* mutant animals showed uncoordinated

© 2008 Nature Publishing Group http://www.nature.com/nsmb

body movement (Unc), compared with only 0.2% embryonic lethality and 0% Unc observed in wild-type animals (**Table 1**). These defects are similar to but substantially weaker than those seen in *ced-9*(*lf*) animals such as the temperature-sensitive *ced-9*(*n1653*) mutant[32] and can be partially suppressed by a weak *ced-3*(*n2438*) mutation, suggesting that these defects result from ectopic cell deaths. Moreover, *csp-3*(*tm2260*) and *csp-3*(*tm2486*) mutations could exacerbate the defects of *ced-9*(*n1653*) animals (**Table 1**), resulting in almost complete sterility and lethality, suggesting that both genes are important for animal viability.

CSP-3 is widely expressed during *C. elegans* development

To examine the expression pattern of *csp-3*, we generated a *csp-3::gfp* translational fusion ($P_{csp\text{-}3}$*csp-3::gfp*) that contains 4,149 bp of the *csp-3* promoter (**Fig. 1b**). This fusion construct fully rescued the missing cell phenotype of the *csp-3* mutants (**Fig. 2d**), suggesting that the fusion protein is expressed in the right cells and targeted to the appropriate cellular location. CSP-3 is widely expressed in all cells of *C. elegans* embryos, and its expression persists through the larval stages (**Fig. 1d** and data not shown). CSP-3::GFP localizes in the cytoplasm and is excluded from the nucleus (**Fig. 1d**). The localization and expression patterns of CSP-3 are consistent with its role in protecting cells that normally live from apoptosis.

CSP-3 associates with CED-3

Given the sequence similarity between CSP-3 and the small subunit of CED-3, we tested whether CSP-3 associates with CED-3 *in vitro*. We coexpressed the CED-3 zymogen tagged with a Flag epitode and a glutathione-*S*-transferase (GST) CSP-3 fusion in bacteria and carried out GST-fusion protein pull-down assays. Under the condition of limited induction of protein expression, CED-3 existed as an unprocessed zymogen, and GST–CSP-3, but not GST, specifically pulled down the CED-3 zymogen (**Fig. 4a**).

We further characterized the interaction between CSP-3 and CED-3 by examining the binding of CSP-3 to different domains of the CED-3 zymogen (**Fig. 4b**). We found that the large subunit of CED-3 was sufficient to mediate binding to CSP-3, whereas the N-terminal prodomain and the small subunit of CED-3 did not show detectable binding to CSP-3 (**Fig. 4b** and data not shown). These results suggest that CSP-3 may mimic the small subunit of CED-3 to interact with the large subunit of CED-3 and thus interfere with the proapoptotic function of CED-3.

We also examined whether CSP-3 associates with CED-3 *in vivo* by performing co-immunoprecipitation assays using an integrated transgene (*smIs10*) carrying a *ced-3::gfp* translational fusion ($P_{ced\text{-}3}$*ced-3::gfp*). *smIs10* can fully rescue the cell-death defect of

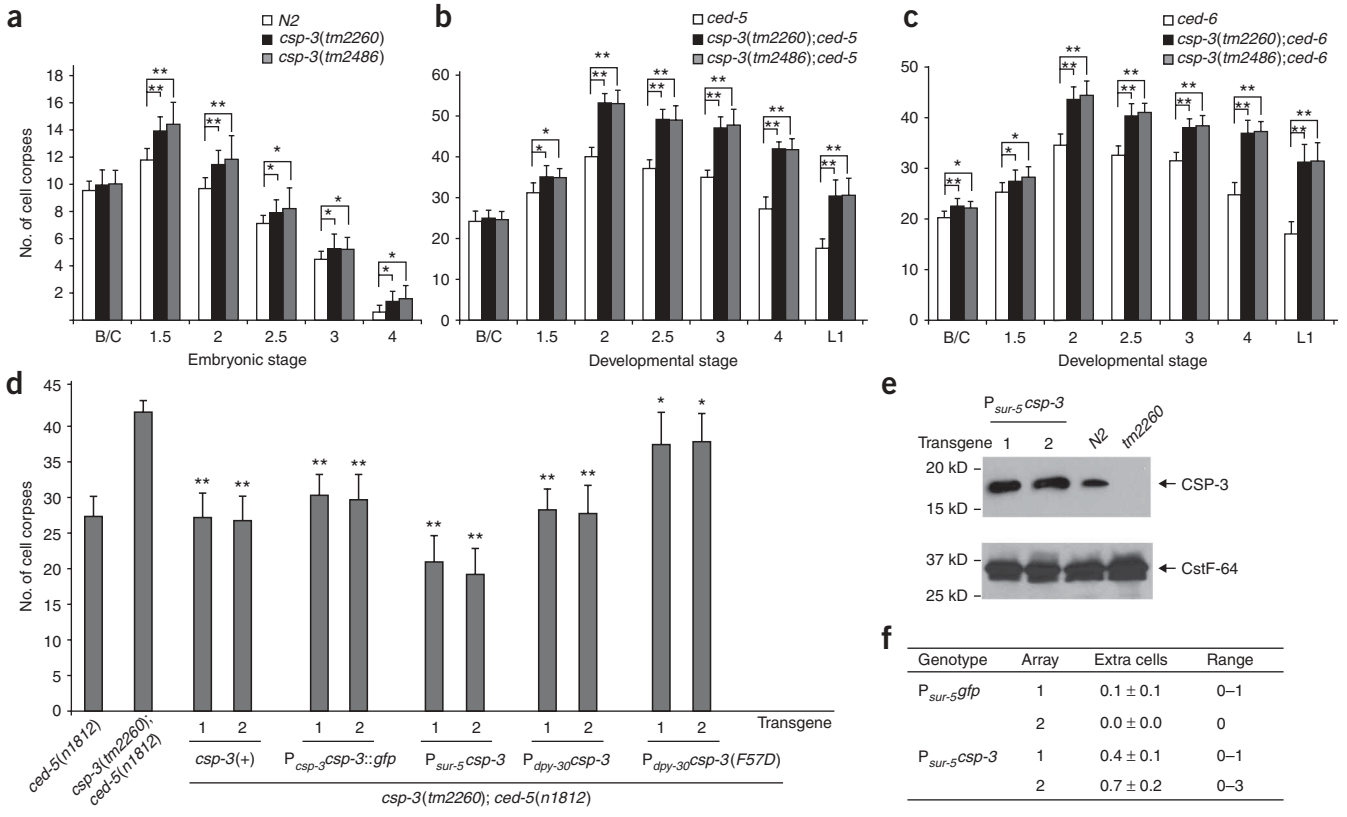

f

Genotype	Array	Extra cells	Range
$P_{sur\text{-}5}$*gfp*	1	0.1 ± 0.1	0–1
	2	0.0 ± 0.0	0
$P_{sur\text{-}5}$*csp-3*	1	0.4 ± 0.1	0–1
	2	0.7 ± 0.2	0–3

Figure 2 Loss of *csp-3* results in increased cell deaths during embryonic development. (**a**–**c**) Cell corpses were scored in the indicated strains. *ced-5*(*n1812*) and *ced-6*(*n2096*) alleles were used in **b** and **c**, respectively. Bean (B/C), 1.5-fold (1.5), 2.0-fold (2), 2.5-fold (2.5), 3.0-fold (3), 4.0-fold (4) –stage embryos and L1 larvae (L1) were examined. (**d**) Rescue of the *csp-3* mutant by various transgenes. Four-fold stage embryos from *csp-3*(*tm2260*);*ced-5*(*n1812*) animals carrying the indicated transgenes were scored for cell corpses. In **a**–**d**, the *y*-axis represents the average number of cell corpses scored. Error bars are s.d. Fifteen embryos or larvae were scored for each stage or transgenic line. In **a**–**c**, the significance of differences between different genetic backgrounds was determined by analysis of variance and Fisher probable least-squares difference. *, $P < 0.05$; **, $P < 0.0001$. All other points had *P* values > 0.05. In **d**, data from two independent transgenic lines were analyzed similarly and compared with that of *csp-3*(*tm2260*);*ced-5*(*n1812*) animals. *, $P < 0.05$; **, $P < 0.0001$. (**e**) Western blot analysis of the expression levels of CSP-3 in two $P_{sur\text{-}5}$*csp-3* transgenic lines (line 1 and lines 2) compared with that of wild-type animals (N2) or *csp-3*(*tm2260*) animals. (**f**) Overexpression of CSP-3 in *C. elegans* mildly inhibits programmed cell death. Extra undead cells in the anterior pharynx were scored in two $P_{sur\text{-}5}$*csp-3* transgenic lines and two control $P_{sur\text{-}5}$*gfp* transgenic lines. At least 15 transgenic animals were scored for each strain.

© 2008 Nature Publishing Group http://www.nature.com/nsmb

© 2008 Nature Publishing Group http://www.nature.com/nsmb

a

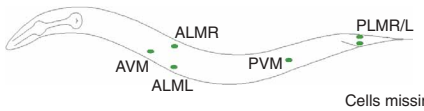

Genotype	Cells missing (%) AVM	ALM	PVM	PLM
bzIs8	0%	0.5%	0%	0%
csp-3(*tm2260*); *bzIs8*	2.0%	10.0%	6.0%	4.0%
csp-3(*tm2486*); *bzIs8*	3.0%	9.5%	4.0%	5.0%
csp-3(*tm2260*); *ced-3*(*n2433*); *bzIs8*	0%	0.5%	0%	0%
csp-3(*tm2486*); *ced-3*(*n2433*); *bzIs8*	0%	0.5%	0%	0.5%
csp-3(*tm2260*); *egl-1*(*n3082*); *bzIs8*	0%	1.0%	0%	0%
csp-3(*tm2486*); *egl-1*(*n3082*); *bzIs8*	0%	1.0%	0%	0%
csp-3(*tm2260*); *ced-4*(*n1162*); *bzIs8*	0%	0.5%	0%	0.5%
csp-3(*tm2486*); *ced-4*(*n1162*); *bzIs8*	0%	1.0%	0%	0%

b

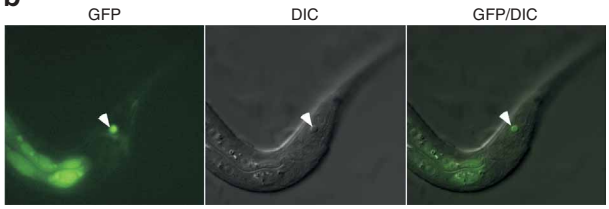

c

Genotype	Animals missing at least one touch cell (%)
bzIs8	1%
csp-3(*tm2260*); *bzIs8*	30%
csp-3(*tm2260*); *bzIs8*; *Ex*[*csp-3*(+)]#1	2%
csp-3(*tm2260*); *bzIs8*; *Ex*[*csp-3*(+)]#2	3%
csp-3(*tm2260*); *bzIs8*; *Ex*[*csp-3*(+)]#3	2%

d

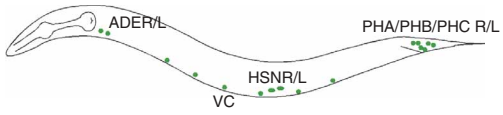

Strain	Cells missing (%) ADE	VC	HSN	PH	Animals missing 1 neuron (%)
inIs179	0%	0%	0%	0.3%	2%
csp-3(*tm2260*); *inIs179*	3.0%	2.3%	0.5%	4.8%	39%
csp-3(*tm2486*); *inIs179*	2.0%	2.0%	0.5%	4.2%	37%
csp-3(*tm2260*); *inIs179*; *ced-3*(*n2433*)	0%	0%	0%	0.5%	3%
csp-3(*tm2486*); *inIs179*; *ced-3*(*n2433*)	0%	0%	0%	0.3%	2%

Figure 3 Loss of *csp-3* causes cells that normally live to undergo programmed cell death. (**a**) Touch receptor neurons are randomly lost in *csp-3* mutants via programmed cell death. An integrated transgene (*bzIs8*) was used to monitor the survival of six touch receptor neurons (green circles) as described in Methods. The percentage of a specific touch-cell type lost was shown. At least 100 animals were scored for each strain. ALML, anterior lateral microtubule cell left; ALMR, anterior lateral microtubule cell right; AVM, anterior ventral microtubule cell; PLML, posterior lateral microtubule cell left; PLMR, posterior lateral microtubule cell right; PVM, posterior ventral microtubule cell. (**b**) A PLM neuron labeled by GFP in a *csp-3*(*tm2260*);*ced-5*(*n1812*);*bzIs8* larva undergoes ectopic cell death and adopts a raised-button–like morphology characteristic of apoptotic cells (indicated by an arrowhead). (**c**) The *csp-3(+)* transgene rescues the missing cell defect of the *csp-3*(*tm2260*) mutant. Touch cells were scored as described in **a**. The percentage of animals missing at least one touch cell is shown. Ex, extrachromosomal transgenic array. (**d**) Several different types of neurons are also randomly lost in *csp-3* mutants. An integrated transgene (*inIs179*) was used to label 16 neurons (green circles) in all strains examined. The presence of these neurons in L4 larvae was scored by epifluorescence microscopy. The percentage of a specific cell type missing was calculated as follows: the number of cells missing in a cell type divided by the number of total cells expected in a cell type. The specific cell types are: two ADE neurons, six ventral cord neurons (VC), two HSN neurons, six phasmid (PH) neurons (two PHA, two PHB and two PHC). The percentage of animals missing at least one neuron is also shown. At least 100 animals were scored for each strain.

the *ced-3*(*lf*) mutants (**Supplementary Table 2** online), suggesting that the CED-3::GFP fusion is functional. Using a monoclonal antibody to GFP, we coprecipitated the CED-3::GFP from the lysate of *smIs10* animals (**Fig. 4c**). In contrast, no CSP-3 was coprecipitated with another GFP fusion, CEH-30::GFP[33], from the lysate of *smIs54* animals, which carry the *ceh-30::gfp* translational fusion (**Fig. 4c**). Therefore, CSP-3 physically associates with CED-3 both *in vitro* and *in vivo*.

To identify CSP-3 residues that are important for binding to CED-3, we constructed a three-dimensional structural model of the CED-3 large subunit–CSP-3 complex based on the crystal structure of active caspase-3 (ref. 34 and **Supplementary Fig. 1a** online). Several single amino acid substitutions (F57D, I76D, A87E and L30E) were generated in CSP-3 using the modeled complex as a guideline and assessed for their abilities to affect CSP-3 binding to CED-3 *in vitro* (data no shown). Alteration of one relatively conserved residue, Phe57, in CSP-3 to aspartic acid (F57D; **Fig. 1a**) markedly reduced the binding of CSP-3 to the CED-3 zymogen or the large subunit of CED-3 *in vitro* (**Fig. 4a,b**). Notably, transgenes expressing this CSP-3(F57D) mutant ($P_{dpy\text{-}30}$CSP-3(F57D)) could hardly rescue the ectopic cell death defect of the *csp-3* mutant, whereas transgenes

Table 1 The *csp-3* mutations cause embryonic lethality and uncoordinated body movement

Genotype	Eggs laid per animal[a]	Embryonic lethality (%)[a]	Uncoordinated (%)[a]
N2	209 ± 13.0	0.2 ± 0.1	0.0 ± 0.0
csp-3(*tm2260*)	152 ± 7.9	5.0 ± 0.3[b]	2.1 ± 1.0[c]
csp-3(*tm2486*)	155 ± 9.4	5.9 ± 0.3[b]	1.7 ± 0.7[c]
ced-9(*n1653ts*)	10.7 ± 2.5	20.4 ± 1.5	ND[d]
ced-3(*n2438*)	166 ± 4.5	1.0 ± 0.4	0.0 ± 0.0
csp-3(*tm2260*); *ced-3*(*n2438*)	157 ± 12.6	1.6 ± 0.2	0.6 ± 0.2
csp-3(*tm2486*); *ced-3*(*n2438*)	158 ± 13.4	1.5 ± 0.2	0.7 ± 0.1
csp-3(*tm2260*); *ced-9*(*n1653ts*)	0.8 ± 0.5	58.7 ± 5.5	ND[d]
csp-3(*tm2486*); *ced-9*(*n1653ts*)	0.9 ± 0.3	59.6 ± 5.1	ND[d]
ced-9(*n1653ts*); *smIs179*	12 ± 2.5	17.6 ± 1.9	ND[d]
csp-3(*tm2260*); *ced-9*(*n1653ts*); *smIs179*	6.8 ± 2.0	37.9 ± 2.3	ND[d]

[a]All strains were maintained at 25 °C. The number of eggs laid by hermaphrodite animals, the number of eggs that hatched and the number of animals that showed uncoordinated body movement were scored as described in Methods. The percentage of embryonic lethality was scored as the fraction of eggs laid that did not hatch[32]. Strong loss-of-function mutations in *ced-3* or *ced-4* also cause some embryonic lethality[32] and thus cannot be used to suppress embryonic lethality of *csp-3(lf)* embryos. *smIs179* is an integrated transgene containing the $P_{csp\text{-}3}$*flag::csp-3* construct that rescues the missing cell defect of the *csp-3* mutants (data not shown). Data shown are mean ± s.d. and are derived from three independent experiments. For results shown in the second and third columns, 20 animals were scored in each experiment. For results shown in the fourth column, at least 90 animals were scored in each experiment. [b]Compared with N2 animals, $P < 0.001$ (two-tail Student *t*-test). Compared with *csp-3(lf); ced-3(n2438)* animals, $P < 0.005$. [c]Compared with N2 animals, $P < 0.01$. Compared with *csp-3(lf); ced-3(n2438)* animals, $P < 0.05$. [d]ND, not determined. *ced-9(n1653)* animals are sick at 25 °C and the Unc phenotype cannot be reliably scored.

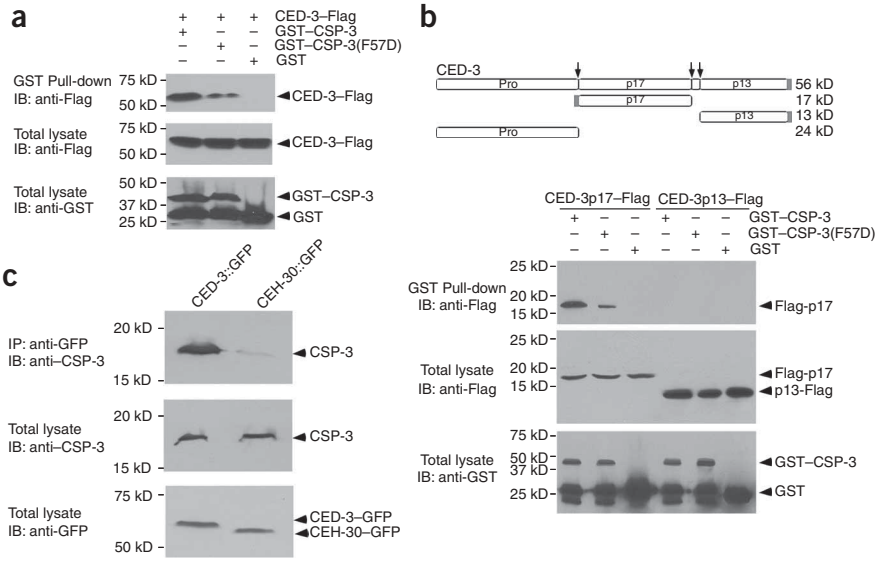

Figure 4 CSP-3 associates with CED-3 *in vitro* and in *C. elegans*. (**a**) CSP-3 binds to the CED-3 zymogen. GST–CSP-3, GST–CSP-3(F57D) or GST was coexpressed in bacteria with the CED-3 zymogen tagged with a Flag epitode (CED-3–Flag). One portion of the soluble fraction was analyzed by western blot (IB) to examine the expression levels of GST fusion proteins and CED-3–Flag. The remaining portion of the soluble fraction was used for GST protein pull-down experiment, and the amount of CED-3–Flag pulled down was analyzed by western blot analysis. (**b**) CSP-3 associates specifically with the large subunit of CED-3 *in vitro*. GST–CSP-3, GST–CSP-3(F57D) or GST was coexpressed in bacteria with the CED-3 large subunit (p17) or the small subunit (p13), both tagged with a Flag epitode (gray box). Analysis of expression levels as well as the amounts of two CED-3 subunits coprecipitated with GST fusion proteins was conducted as described in **a**. The diagram above depicts the domain structure of the CED-3 zymogen, with arrows indicating the three proteolytic cleavage sites that lead to the activation of the CED-3 zymogen. The three CED-3 cleavage products are shown below as boxes. (**c**) CSP-3 associates with CED-3 in *C. elegans*. Lysates from *C. elegans* animals expressing CED-3::GFP or CEH-30::GFP were prepared as described in Methods. One portion of the worm lysate was used in the western blot analysis to examine the expression levels of CSP-3 and GFP fusion proteins. The remaining portion of the lysate was incubated with a mouse anti-GFP monoclonal antibody and precipitated using Protein G Sepharose beads. The amount of the CSP-3 protein pulled down with the GFP fusion proteins was analyzed by western blot using purified anti–CSP-3 antibody. A small amount of full-length CED-3::GFP fusion was detected in the lysate (data not shown). The predominant species detected was CED-3::GFP fusion without its prodomain but containing both large and small subunits.

© 2008 Nature Publishing Group http://www.nature.com/nsmb

expressing the wild-type CSP-3 protein ($P_{dpy\text{-}30}$CSP-3) at a similar level were able to do so (**Fig. 2d** and **Supplementary Fig. 1b**). These results indicate that association of CSP-3 with CED-3 is important for CSP-3 to protect cells that normally live from apoptosis.

CSP-3 inhibits autoactivation of the CED-3 zymogen

The association of CSP-3 with CED-3 may interfere with either the activation of the CED-3 zymogen or the activity of the activated CED-3 protease, or both. We first tested whether CSP-3 blocks the autoactivation of the CED-3 zymogen using an *in vitro* assay described previously[14]. In this assay, the CED-3 zymogen synthesized in the rabbit reticulocyte lysate first existed as an unprocessed precursor and was then slowly autoprocessed into active forms (**Fig. 5a**, lanes 1–3). The autoactivation of the CED-3 zymogen was inhibited by the addition of the GST–CSP-3 protein (**Fig. 5a**, lanes 4–6) but not affected by addition of a similar amount of the GST–CSP-3(F57D) or GST protein (**Fig. 5a**, lanes 1–3 and 7–9).

We next examined whether CSP-3 may inhibit the activation of the CED-3 zymogen mediated by oligomeric CED-4 (ref. 14; **Fig. 5b**). Oligomeric CED-4 accelerated CED-3 maturation (**Fig. 5b**, lanes 6–10), leading to the activation of CED-3 at the 30-min time point, when there was no sign of CED-3 autoactivation (compare lanes 1 and 6 in **Figure 5b**). Although GST–CSP-3 completely inhibited CED-3 autoactivation (**Fig. 5b**, lanes 11–15), it delayed but did not block the activation of CED-3 induced by oligomeric CED-4 (**Fig. 5b**, lanes 16–20), as by the 180-min or 230-min time point (lanes 19 and 20) CED-3 was activated to the same extent as seen in CED-3 autoactivation at the 180-min or 230-min time point (lanes 4 and 5) or that seen in CED-4–mediated CED-3 activation at the 80-min or later time points (lanes 7–10). We confirmed this observation by adding oligomeric CED-4 to a preformed GST–CSP-3–CED-3 zymogen complex and found that oligomeric CED-4, but not the nonapoptotic CED-4 monomer[14], induced the proteolytic activation of the CED-3 zymogen (**Fig. 5c**). These results suggest that CSP-3 inhibits the autoactivation of CED-3 but is unable to block CED-4–mediated CED-3 activation, consistent with the observation that CSP-3 protects cells that normally live but fails to block the death of cells that are programmed to die where oligomeric CED-4 is formed.

On the other hand, when GST–CSP-3 was coexpressed with the CED-3 zymogen during the CED-3 activation process or incubated with the activated CED-3 protease (acCED-3), it failed to inhibit the cleavage of CED-9, an endogenous CED-3 substrate[35], by active CED-3 (**Fig. 5d** and **Supplementary Fig. 2** online). This result suggests that, once the active CED-3 heterodimeric complex is formed, active CED-3 is resistant to the inhibition of CSP-3.

DISCUSSION

In this study, we show that loss of *csp-3* in *C. elegans* causes ectopic deaths of cells that normally live, indicating that *csp-3* acts as a cell-death inhibitor to protect cells from apoptosis. CSP-3 shares sequence similarity to the small subunit of CED-3 and can associate with the CED-3 zymogen through its large subunit. *In vitro* CSP-3 inhibits the autoactivation of the CED-3 zymogen but does not block CED-4–mediated CED-3 activation or the catalytic activity of the activated CED-3 caspase. A mutation in CSP-3 (F57D) that weakens the binding of CSP-3 to CED-3 markedly reduces its ability to inhibit the autoactivation of the CED-3 zymogen *in vitro* and to protect against cell death in *C. elegans*. Altogether, these findings suggest that CSP-3 is a protein inhibitor of the *C. elegans* CED-3 caspase and specifically suppresses the autoactivation of the CED-3 zymogen.

Our results are consistent with a model in which CSP-3 binds to the CED-3 zymogen and prevents inadvertent CED-3 autoactivation through homodimerization in cells that normally live (**Fig. 5e**). In cells that are programmed to die, EGL-1 binds to the cell-death inhibitor CED-9 and triggers CED-4 disassociation and oligomerization[14,25]. Oligomeric CED-4 then overrides CSP-3 inhibition by forcing the dimerization or oligomerization of the CED-3 zymogen and subsequent CED-3 proteolytic activation[3,14,25] (**Fig. 5e**),

as oligomeric CED-4, but not monomeric CED-4, is sufficient to induce CED-3 activation from a purified CSP-3–CED-3 zymogen inhibitory complex *in vitro* (**Fig. 5c**). Oligomeric CED-4 may achieve this by binding to the CED-3 zymogen and inducing a CED-3 conformational change that reduces CED-3 binding to CSP-3. Alternatively, CED-4 may compete with CSP-3 for binding to the CED-3 zymogen. In either case, CSP-3 can delay CED-4–mediated activation of CED-3 *in vitro* (**Fig. 5b**), causing mild inhibition of programmed cell death *in vivo* when overexpressed (**Fig. 2f**). Using this unique mechanism, CSP-3 is able to safeguard against inadvertent CED-3 autoactivation in cells that normally live, and at the same time does not interfere with normal programmed cell death (**Fig. 5e**).

Given the importance of caspases in cell killing and the presence of caspase inhibitors, such as the IAP family of apoptosis inhibitors with crucial roles in regulating apoptosis activation[16,22], in both mammals and fruitflies, it is surprising that no direct caspase inhibitor had been identified previously in *C. elegans* and it was unclear how the activity of CED-3 is tightly controlled in cells that normally live. The identification of CSP-3 as a novel CED-3 inhibitor provides an answer to this enigma. However, given the relatively weak phenotype of the *csp-3* mutants and the presence of multiple IAP proteins that seem to act redundantly to protect against cell death in mammals and fruitflies[17–23,36], it is possible that additional cell-death or caspase inhibitors exist and act redundantly with CSP-3 and CED-9 to safeguard the survival of cells that should live in *C. elegans*.

Our study reveals a previously unreported mechanism by which caspase activation can be regulated in general. We suggest that there are CSP-3–like partial caspase homologs in mammals that negatively regulate the activation of caspases by forming inactive heterodimers with functional caspases. These CSP-3–like caspase inhibitors may thus act redundantly with IAP proteins to inhibit apoptosis[36]. CSP-3–like proteins could also arise from alternative splicing of the functional caspase genes, as in the case of the caspase-2 gene, which encodes two alternatively spliced products: a long form (caspase-2L) and a short form (caspase-2S)[37]. Caspase-2S contains only the prodomain and the large subunit of caspase-2L. When caspase-2S is overexpressed in Rat-1 cells, it inhibits apoptosis induced by serum deprivation[37]. It is conceivable that caspase-2S may do so by binding to the small subunit of the caspase-2 zymogen or similar regions of other caspases through its large subunit and forming inactive heterodimers. Alternatively, caspase-2S may compete with the caspase-2 zymogen for binding to the caspase-2 activator. In either case, caspase-2S can block

© 2008 Nature Publishing Group http://www.nature.com/nsmb

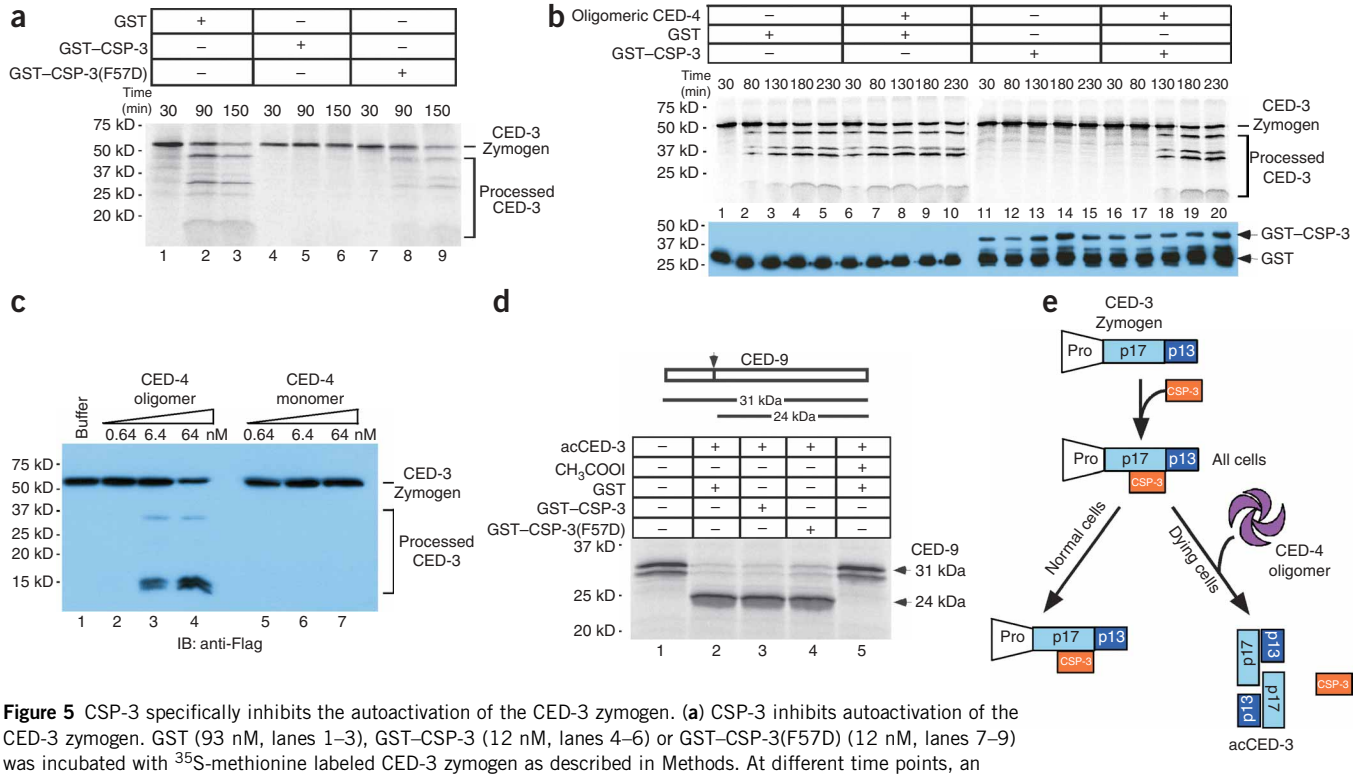

Figure 5 CSP-3 specifically inhibits the autoactivation of the CED-3 zymogen. (**a**) CSP-3 inhibits autoactivation of the CED-3 zymogen. GST (93 nM, lanes 1–3), GST–CSP-3 (12 nM, lanes 4–6) or GST–CSP-3(F57D) (12 nM, lanes 7–9) was incubated with ^{35}S-methionine labeled CED-3 zymogen as described in Methods. At different time points, an aliquot was taken out and SDS sampling buffer was added to stop the reaction. The samples were resolved by 15% SDS-PAGE and subjected to autoradiography. (**b**) CSP-3 delays but does not block CED-4–mediated activation of CED-3. GST (93 nM) or GST–CSP-3 (12 nM) was incubated with ^{35}S-methionine labeled CED-3 zymogen in the absence or presence of oligomeric CED-4 (40 nM) (added 20 min later). At different time points, an aliquot was taken out and SDS sampling buffer was added. One half of the aliquot was resolved by 15% SDS-PAGE and subjected to autoradiography (above). One-fourth of the aliquot was used for the immunoblotting analysis using an anti-GST antibody (below). (**c**) Oligomeric CED-4 overrides CSP-3 inhibition to induce CED-3 activation. Preformed GST-CSP-3–CED-3-Flag complexes (~70 nM of CED-3–Flag) were incubated either with buffer or with increasing concentrations of oligomeric or monomeric CED-4 at 30 °C for 30 min (Methods), before being resolved on 15% SDS-PAGE and detected with an anti-Flag antibody. (**d**) CSP-3 does not inhibit the activity of the active CED-3 protease *in vitro*. CED-3–Flag was coexpressed with GST, GST–CSP-3 or GST–CSP-3(F57D) for 3 h in bacteria. The bacterial lysate containing similar levels of active CED-3 (acCED-3) and GST fusion proteins (**Supplementary Fig. 2b**) was incubated with ^{35}S-methionine–labeled CED-9 for 2 h at 30 °C. In one reaction, the caspase inhibitor iodoacetic acid (5 mM) was included. The reactions were resolved by 15% SDS-PAGE and detected by autoradiography. (**e**) A CSP-3 working model in *C. elegans*. CSP-3 associates with the CED-3 zymogen in all cells. In cells that normally live, CSP-3 prevents the CED-3 zymogen from dimerization and inadvertent autoactivation. In cells that are programmed to die, CED-4 oligomer overrides CSP-3 inhibition to induce the activation of the CED-3 zymogen via the proximity-induced dimerization model[6].

homodimerization of the caspase-2 zymogen needed for its activation, but is unlikely to affect the activity of the activated caspase.

METHODS

Strains. We cultured strains of *C. elegans* at 20 °C using standard procedures[38], unless otherwise noticed. The N2 Bristol strain was used as the wild-type strain. Most of the alleles used in this study have been described previously[39], except *csp-3*(*tm2260*), *csp-3*(*tm2486*), *inIs179*, *smIs179* and *bzIs8*. *bzIs8* is an integrated transgene located on LG X and contains a $P_{mec\text{-}4}$*gfp* construct[30], which directs GFP expression in six *C. elegans* touch receptor neurons. *inIs179* is an integrated transgenic array located on LG II and contains a $P_{ida\text{-}1}$*::gfp* construct[31], which directs GFP expression in the phasmid neurons (PHA, PHB and PHC), ventral cord neurons (VC), hermaphrodite-specific neurons (HSN) and ADE neurons.

Isolation of *csp-3*(*tm2260*) and *csp-3*(*tm2486*) deletion alleles. We isolated the *csp-3*(*tm2260*) and *csp-3*(*tm2486*) deletion alleles from trimethylpsoralen (TMP) and UV-mutagenized worms[40]. The nested primers used to screen for the *csp-3*(*tm2260*) and *csp-3*(*tm2486*) alleles by PCR were 5′-CGCCTCAAACGC CACTGGAT-3′ and 5′-GCTAGCATGACATCGTCACA-3′ for the first-round amplification and 5′-ATTCATCGTAGCAGCGGGAA-3′ and 5′-CGCCACTG GATTCTCTGGTA-3′ for the second-round amplification. Both mutants were backcrossed with wild-type (N2) animals at least six times before they were analyzed further.

Counting of cells in the anterior pharynx and apoptotic cell corpses. We counted nuclei in the anterior pharynx of L4 larvae and cell corpses in animals at various embryonic and larval stages using Nomarski optics as previously described[41].

Quantification of cells labeled with GFP. We identified cells derived from various lineages with the aid of integrated transgenes that express GFP in different cell types. L4 larval animals were scored for missing cells using Nomarski optics equipped with epifluorescence.

Assays for embryonic lethality and other developmental abnormalities. We transferred hermaphrodite animals to fresh plates every 12 h and counted the number of eggs that they laid and the number of embryos that hatched as described previously[32]. Animals were also scored for uncoordinated body movement (Unc) and egg-laying deficiency (Egl).

Molecular biology. Standard methods of cloning, sequencing and PCR were used. We generated the $P_{csp\text{-}3}$*csp-3::gfp* fusion construct by inserting a *csp-3* minigene containing 4,149 bp of the *csp-3* promoter and the full-length *csp-3* cDNA into the pPD95.77 vector. We obtained the full-length *csp-3* cDNA using reverse-transcription PCR (RT-PCR). The *csp-3* cDNA clone containing the F57D substitution was generated using a QuikChange Site-Directed Mutagenesis kit (Stratagene) and confirmed by DNA sequencing.

Transgenic animals. We performed germline transformation as described previously[41]. The $P_{sur\text{-}5}$*csp-3*, $P_{dpy\text{-}30}$*csp-3*, $P_{dpy\text{-}30}$*csp-3*(F57D) or *csp-3*(+) construct (at 25 ng μl^{-1} each) was injected into animals with the appropriate genetic background using $P_{sur\text{-}5}$*gfp* (25 ng μl^{-1}) as a co-injection marker, which directs GFP expression in all somatic cells. The $P_{csp\text{-}3}$*csp-3::gfp* translational fusion construct (at 25 ng μl^{-1}) was injected into *csp-3*(*tm2260*); *ced-5*(*n1812*) animals with pRF4 (at 50 ng μl^{-1}), a dominant *rol-6* construct, as a co-injection marker.

Expression and purification of the CSP-3 and CED-3 proteins. We generated all protein-expression constructs using the standard PCR-based cloning strategy and verified the clones through sequencing. CSP-3 and CED-3 proteins were expressed either individually or together in *Escherichia coli* strain BL21(DE3) as an N-terminally tagged GST fusion protein and a C-terminally Flag-tagged protein using a pGEX-4T-2 vector (Pharmacia) and a pET-3a vector (Novagen), respectively. The soluble fraction of the *E. coli* lysate expressing GST–CSP-3 proteins (wild-type or F57D) was purified using a glutathione Sepharose column and eluted with 10 mM reduced glutathione (Amersham).

GST fusion protein pull-down assays. The GST–CSP-3 fusion protein (wild-type or F57D) or GST was coexpressed with CED-3–Flag, CED-3p13–Flag, or Flag-CED-3p17 in BL21(DE3). Bacteria were lysed by sonication in the lysis buffer (50 mM Tris, pH 8.0, 0.5 mM EDTA, 150mM NaCl, 0.01% (v/v) Triton X-100 and 0.5 mM sucrose) with protease inhibitors, and the soluble fraction was incubated with glutathione Sepharose beads at 4 °C for 2 h. The Sepharose beads were then washed five times with the same buffer before the proteins were resolved on a 15% (w/v) SDS polyacrylamide gel (SDS-PAGE), transferred to a PVDF membrane and detected by immunoblotting with an anti-Flag antibody (Sigma). For the CED-4–mediated CED-3 activation assay, the Sepharose beads tethered with GST–CSP-3–CED-3–Flag complexes were washed with CED-3 buffer (100 mM Tris, pH 8.0, 250 mM NaCl, 0.1% (v/v) NP-40, 5 mM DTT, 0.5 mM sucrose and 10% (v/v) glycerol) and then incubated with increasing concentrations of oligomeric or monomeric CED-4, prepared as described previously[14], at 30 °C for 30 min with occasional shaking, before they were resolved on 15% (w/v) SDS-PAGE and detected by immunoblotting with an anti-Flag antibody. To measure the concentration of the CED-3 zymogen in the pull-down samples, GST fusion pull-down samples were resolved on the SDS polyacrylamide gel together with a series of BSA proteins with increasing concentrations. The gel was then stained with Coomassie Blue and the concentration of the CED-3 zymogen was estimated by comparing the intensity of the CED-3 band with that of various BSA bands with different concentrations.

***In vitro* CED-3 zymogen activation assay.** The CED-3 zymogen was first synthesized and labeled with ^{35}S-methionine in the TNT Transcription/Translation coupled system (Promega) at 30 °C as described previously[14], in the presence of an equal amount of GST–CSP-3, GST–CSP-3(F57D) or GST. An aliquot of the reaction was taken out at different time points and mixed with SDS sampling buffer to stop the reaction. For the CED-4–mediated CED-3 activation assay, oligomeric CED-4 was added 20 min after the initiation of the translation reaction. An aliquot of the reaction was then taken out at different time points and mixed with SDS sampling buffer to stop the reaction. All samples were resolved by 15% (w/v) SDS–PAGE and analyzed by autoradiography.

***In vitro* CED-3 activity assays.** CED-9 was synthesized and labeled with ^{35}S-methionine in the TNT Transcription/Translation coupled system (Promega) and used as a CED-3 substrate for *in vitro* CED-3 protease activity assays. The CED-3 zymogen was coexpressed with GST–CSP-3, GST–CSP-3(F57D) or GST for 3 h in bacteria. The bacterial lysate containing similar amounts of active CED-3 and GST fusion proteins was incubated with ^{35}S-methionine–labeled CED-9 for 2 h at 30 °C as described previously[42]. The reactions were then resolved by 15% (w/v) SDS–PAGE and analyzed by autoradiography.

***In vivo* co-immunoprecipitation assay.** We cultured *C. elegans* animals carrying the integrated transgene *smIs10* ($P_{ced\text{-}3}$*ced-3::gfp*) or *smIs54* ($P_{ceh\text{-}30}$*ceh-30::gfp*) in liquid medium for 48 h. The animals were harvested and washed three times with 100 mM KCl. Bacteria and fungi were removed by sucrose gradient centrifugation. The animals were then lysed by sonication in the lysis buffer (20 mM HEPES, 100 mM KCl, 0.5% (v/v) NP-40, 1 mM EDTA and 1 mM DTT) with protease inhibitors, and the soluble fraction was precleared with Protein-G Sepharose beads (Pharmarcia). Subsequently, the precleared worm lysate was incubated at 4 °C with a monoclonal anti-GFP antibody (3E6, Qbiogene) for 1 h with gentle shaking. Protein-G Sepharose beads were then added and incubation was continued for another 2 h. The resins were then washed five times with the lysis buffer before the proteins were resolved on a 15% (w/v) SDS-PAGE, transferred to a PVDF membrane, and detected by immunoblotting using an anti–CSP-3 antibody.

Generation and purification of anti–CSP-3 antibodies. We purified the recombinant GST–CSP-3 protein from the soluble fraction of the bacterial lysate using Glutathione Sepharose™4B beads as described above and used it to raise polyclonal antibodies against CSP-3 in rats (Spring Valley Laboratories). We then affinity purified 2 ml of terminal bleed using nitrocellulose membrane strips carrying 1 mg of CSP-3–His_6 protein as described in detail previously[41].

© 2008 Nature Publishing Group http://www.nature.com/nsmb

Note: Supplementary information is available on the Nature Structural & Molecular Biology website.

ACKNOWLEDGMENTS

We thank members of the Xue laboratory and N. Yan for comments and discussions, A. Seluzicki for the initial observation, M. Driscoll (Rutgers University) for the *bzIs8* strain, J. Hutton (University of Colorado Health Science Center) for the *inIs179* strain and T. Blumenthal (University of Colorado) for anti–CstF-64 antibody. This work was supported by US National Institutes of Health R01 grants (GM059083 and GM079097 to D.X. and GM072633 to Yigong S.), a Burroughs Welcome Fund Career Award to D.X. and a grant from Ministry of Education, Culture, Sports, Science and Technology (MEXT) of Japan to S.M. X.G. is supported by University of Colorado Matching Grant to the SCR Training Grant (T32 GM08759).

AUTHOR CONTRIBUTIONS

X.G. performed most of the experiments. X.G. and D.X. designed and interpreted all experiments. Yigong S. performed the structural modeling of the CSP-3–CED-3 complex. S.Y. and S.M. isolated *csp-3* deletion alleles. Yong S. and A.N. contributed to some of the experiments. X.G. and D.X. wrote the paper and others commented on the manuscript.

Published online at http://www.nature.com/nsmb/

Reprints and permissions information is available online at http://npg.nature.com/reprintsandpermissions/

© 2008 Nature Publishing Group http://www.nature.com/nsmb

1. Steller, H. Mechanisms and genes of cellular suicide. *Science* **267**, 1445–1449 (1995).
2. Thornberry, N.A. & Lazebnik, Y. Caspases: enemies within. *Science* **281**, 1312–1316 (1998).
3. Boatright, K.M. & Salvesen, G.S. Mechanisms of caspase activation. *Curr. Opin. Cell Biol.* **15**, 725–731 (2003).
4. Shi, Y. Mechanisms of caspase activation and inhibition during apoptosis. *Mol. Cell* **9**, 459–470 (2002).
5. Budihardjo, I., Oliver, H., Lutter, M., Luo, X. & Wang, X. Biochemical pathways of caspase activation during apoptosis. *Annu. Rev. Cell Dev. Biol.* **15**, 269–290 (1999).
6. Degterev, A., Boyce, M. & Yuan, J. A decade of caspases. *Oncogene* **22**, 8543–8567 (2003).
7. Zou, H., Henzel, W.J., Liu, X., Lutschg, A. & Wang, X. APAF-1, a human protein homologous to *C. elegans* CED-4, participates in cytochrome *c*-dependent activation of caspase-3. *Cell* **90**, 405–413 (1997).
8. Zou, H., Li, Y., Liu, X. & Wang, X. An APAF-1.cytochrome *c* multimeric complex is a functional apoptosome that activates procaspase-9. *J. Biol. Chem.* **274**, 11549–11556 (1999).
9. Jiang, X. & Wang, X. Cytochrome *c*-mediated apoptosis. *Annu. Rev. Biochem.* **73**, 87–106 (2004).
10. James, C., Gschmeissner, S., Fraser, A. & Evan, G.I. CED-4 induces chromatin condensation in *Schizosaccharomyces pombe* and is inhibited by direct physical association with CED-9. *Curr. Biol.* **7**, 246–252 (1997).
11. Wu, D., Wallen, H.D. & Nunez, G. Interaction and regulation of subcellular localization of CED-4 by CED-9. *Science* **275**, 1126–1129 (1997).
12. Chinnaiyan, A.M., O'Rourke, K., Lane, B.R. & Dixit, V.M. Interaction of CED-4 with CED-3 and CED-9: a molecular framework for cell death. *Science* **275**, 1122–1126 (1997).
13. Chen, F. *et al.* Translocation of *C. elegans* CED-4 to nuclear membranes during programmed cell death. *Science* **287**, 1485–1489 (2000).
14. Yan, N. *et al.* Structure of the CED-4–CED-9 complex provides insights into programmed cell death in *Caenorhabditis elegans*. *Nature* **437**, 831–837 (2005).
15. Cory, S., Huang, D.C. & Adams, J.M. The Bcl-2 family: roles in cell survival and oncogenesis. *Oncogene* **22**, 8590–8607 (2003).
16. Deveraux, Q.L. & Reed, J.C. IAP family proteins—suppressors of apoptosis. *Genes Dev.* **13**, 239–252 (1999).
17. Deveraux, Q.L., Takahashi, R., Salvesen, G.S. & Reed, J.C. X-linked IAP is a direct inhibitor of cell-death proteases. *Nature* **388**, 300–304 (1997).
18. Roy, N., Deveraux, Q.L., Takahashi, R., Salvesen, G.S. & Reed, J.C. The c-IAP-1 and c-IAP-2 proteins are direct inhibitors of specific caspases. *EMBO J.* **16**, 6914–6925 (1997).
19. Deveraux, Q.L. *et al.* IAPs block apoptotic events induced by caspase-8 and cytochrome *c* by direct inhibition of distinct caspases. *EMBO J.* **17**, 2215–2223 (1998).
20. Meier, P., Silke, J., Leevers, S.J. & Evan, G.I. The *Drosophila* caspase DRONC is regulated by DIAP1. *EMBO J.* **19**, 598–611 (2000).
21. Hawkins, C.J., Wang, S.L. & Hay, B.A. A cloning method to identify caspases and their regulators in yeast: identification of *Drosophila* IAP1 as an inhibitor of the *Drosophila* caspase DCP-1. *Proc. Natl. Acad. Sci. USA* **96**, 2885–2890 (1999).
22. Salvesen, G.S. & Duckett, C.S. IAP proteins: blocking the road to death's door. *Nat. Rev. Mol. Cell Biol.* **3**, 401–410 (2002).
23. Callus, B.A. & Vaux, D.L. Caspase inhibitors: viral, cellular and chemical. *Cell Death Differ.* **14**, 73–78 (2007).
24. Srinivasula, S.M. *et al.* A conserved XIAP-interaction motif in caspase-9 and Smac/DIABLO regulates caspase activity and apoptosis. *Nature* **410**, 112–116 (2001).
25. Horvitz, H.R. Genetic control of programmed cell death in the nematode *Caenorhabditis elegans*. *Cancer Res.* **59**, 1701s–1706s (1999).
26. Shaham, S. Identification of multiple *Caenorhabditis elegans* caspases and their potential roles in proteolytic cascades. *J. Biol. Chem.* **273**, 35109–35117 (1998).
27. Reddien, P.W. & Horvitz, H.R. The engulfment process of programmed cell death in *Caenorhabditis elegans*. *Annu. Rev. Cell Dev. Biol.* **20**, 193–221 (2004).
28. Hsu, D.R. & Meyer, B.J. The *dpy-30* gene encodes an essential component of the *Caenorhabditis elegans* dosage compensation machinery. *Genetics* **137**, 999–1018 (1994).
29. Gu, T., Orita, S. & Han, M. *Caenorhabditis elegans* SUR-5, a novel but conserved protein, negatively regulates LET-60 Ras activity during vulval induction. *Mol. Cell. Biol.* **18**, 4556–4564 (1998).
30. Harbinder, S. *et al.* Genetically targeted cell disruption in *Caenorhabditis elegans*. *Proc. Natl. Acad. Sci. USA* **94**, 13128–13133 (1997).
31. Zahn, T.R., Macmorris, M.A., Dong, W., Day, R. & Hutton, J.C. IDA-1, a *Caenorhabditis elegans* homolog of the diabetic autoantigens IA-2 and phogrin, is expressed in peptidergic neurons in the worm. *J. Comp. Neurol.* **429**, 127–143 (2001).
32. Hengartner, M.O., Ellis, R.E. & Horvitz, H.R. *Caenorhabditis elegans* gene *ced-9* protects cells from programmed cell death. *Nature* **356**, 494–499 (1992).
33. Peden, E., Kimberly, E., Gengyo-Ando, K., Mitani, S. & Xue, D. Control of sex-specific apoptosis in *C. elegans* by the BarH homeodomain protein CEH-30 and the transcriptional repressor UNC-37/Groucho. *Genes Dev.* **21**, 3195–3207 (2007).
34. Rotonda, J. *et al.* The three-dimensional structure of apopain/CPP32, a key mediator of apoptosis. *Nat. Struct. Biol.* **3**, 619–625 (1996).
35. Xue, D. & Horvitz, H.R. *Caenorhabditis elegans* CED-9 protein is a bifunctional cell-death inhibitor. *Nature* **390**, 305–308 (1997).
36. Harlin, H., Reffey, S.B., Duckett, C.S., Lindsten, T. & Thompson, C.B. Characterization of XIAP-deficient mice. *Mol. Cell. Biol.* **21**, 3604–3608 (2001).
37. Wang, L., Miura, M., Bergeron, L., Zhu, H. & Yuan, J. *Ich-1*, an *Icelced-3*-related gene, encodes both positive and negative regulators of programmed cell death. *Cell* **78**, 739–750 (1994).
38. Brenner, S. The genetics of *Caenorhabditis elegans*. *Genetics* **77**, 71–94 (1974).
39. Riddle, D.L., Blumenthal, T., Meyer, B.J. & Preiss, J.R. (eds.). *C. elegans II* (Cold Spring Harbor Laboratory Press, Cold Spring Harbor, New York, 1997).
40. Gengyo-Ando, K. & Mitani, S. Characterization of mutations induced by ethyl methanesulfonate, UV, and trimethylpsoralen in the nematode *Caenorhabditis elegans*. *Biochem. Biophys. Res. Commun.* **269**, 64–69 (2000).
41. Wang, X., Yang, C., Chai, J., Shi, Y. & Xue, D. Mechanisms of AIF-mediated apoptotic DNA degradation in *Caenorhabditis elegans*. *Science* **298**, 1587–1592 (2002).
42. Xue, D., Shaham, S. & Horvitz, H.R. The *Caenorhabditis elegans* cell-death protein CED-3 is a cysteine protease with substrate specificities similar to those of the human CPP32 protease. *Genes Dev.* **10**, 1073–1083 (1996).

Inhibition of CED-3 zymogen activation and apoptosis in *Caenorhabditis elegans* by a caspase homolog CSP-3

Xin Geng[1], Yong Shi[1], Akihisha Nakagawa[1], Sawako Yoshina[3], Shohei Mitani[3], Yigong Shi[2], and Ding Xue[1]

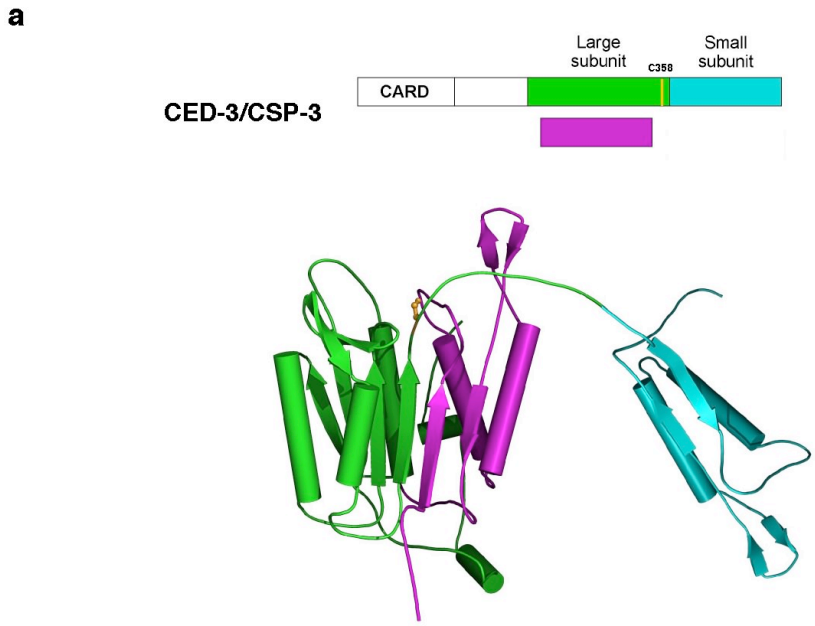

Supplementary Figure 1. (**a**) Three-dimensional structural model of the CED-3/CSP-3 complex. CED-3 large subunit is shown in green, CED-3 small subunit in cyan, and CSP-3 in magenta. CSP-3 complexes with the CED-3 zymogen and blocks CED-3 auto-activation by homodimerization. The crystal structure of caspase-3 (PDB code 1pau) was used as the starting model. Based on the caspase sequence alignment (Fig. 1a), the amino acids in the large and small subunits of caspase-3 are replaced by those in CED-3 and CSP-3, respectively, in the graphics program O. The orientations of side chains were manually adjusted before the modeled structure of the CED-3 large subunit/CSP-3 heterodimer was energy-minimized in program O. **(b)** Western blot analysis of the expression levels of CSP-3 in two $P_{dpy\text{-}30}csp\text{-}3$ transgenic lines and two $P_{dpy\text{-}30}csp\text{-}3(F57D)$ transgenic lines in the *csp-3(tm2260); ced-5(n1812)* mutant background. The CstF-64 protein was used as a loading control.

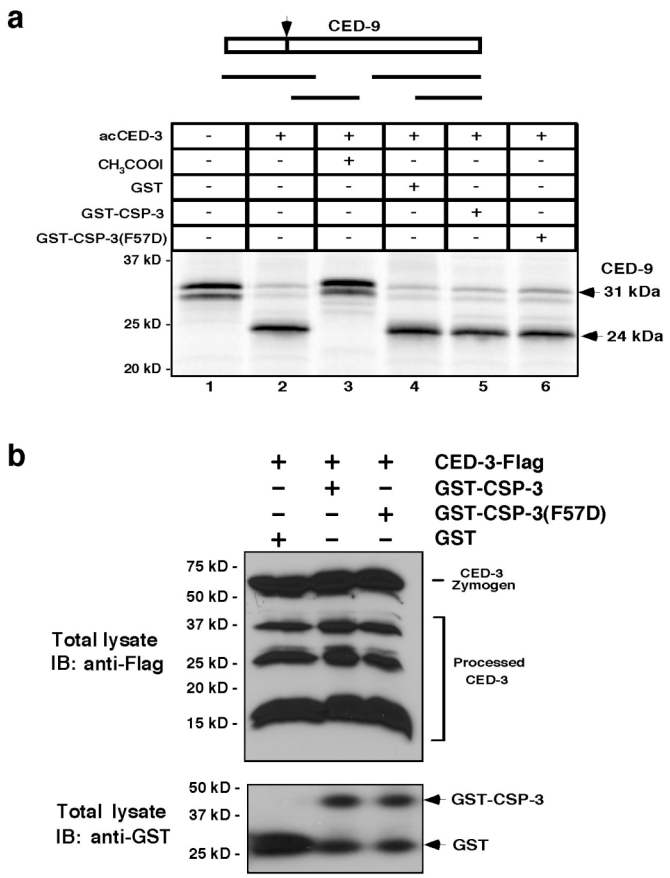

Supplementary Figure 2. CSP-3 does not inhibit the protease activity of the activated CED-3. **(a)** 5 ng of active CED-3 (acCED-3) were incubated with ^{35}S-Methionine-labeled CED-9 and the recombinant proteins (250 ng each) or the caspase inhibitor, iodoacetic acid (5 mM) for 2 h at 30°C. The samples were resolved by 15% SDS-PAGE and subjected to autoradiography. (**b**) Western blot analysis of the expression levels of acCED-3-Flag and GST fusion proteins in the cell lysates used in Figure 5d. The molar ratio of acCED-3 and GST-CSP-3 in the lysate is estimated to be 1:8.

Supplementary Table 1 *csp-3* mutations cause missing cells

Genotype	Extra cell Average [a]	Missing cell Average [a]	% of normal cells missing [b]						
			m2	**I1**	**m1**	**MC**	**NSM**	**I3**	**Others**
N2	0.0 ± 0.0	0.0 ± 0.0	0	0	0	0	0	0	0
csp-3(tm2260)	0.0 ± 0.0	0.5 ± 0.2	0	10	2.5	7.5	0	0	0
csp-3(tm2486)	0.0 ± 0.0	0.6 ± 0.1	0.8	5.0	1.3	12.5	2.5	5.0	0
ced-3(n2438)	1.8 ± 0.3	0.0 ± 0.0	0	0	0	0	0	0	0
csp-3(tm2260); ced-3(n2438)	1.7 ± 0.3	0.3 ± 0.1	0	5.0	0	7.5	0	0	0
csp-3(tm2486); ced-3(n2438)	1.8 ± 0.3	0.4 ± 0.1	0	5.0	3.8	2.5	2.5	0	0

[a] The number of cells that are programmed to die but inappropriately survive (extra cell) or the number of cells that normally live but are missing (missing cell) was scored in the anterior pharynx of L4 hermaphrodites using Nomarski optics. Data shown are mean ± s.e.m. 20 animals were scored in each strain.

[b] The percentage of specific cells in the anterior pharynx that normally live but are missing is shown (the number of missing cells of a specific cell type divided by the total number of specific cells expected). Miss cells were observed in the following cell types: 6 **m2** muscle cells, 2 **I1** neurons, 4 **m1** muscle cells in two ventral planes, 2 **MC** neurons, 2 **NSM** neurons, and one **I3** neuron. Miss cells were not observed in the following cell types (named **others**): 3 **e2** epithelial cells, 3 **e1** epithelial cells, 2 **I2** neurons, one **M4** neuron, one **MI** neuron, and 2 **m1** muscle cells in the dorsal plane.

Supplementary Table 2 The *smIs10* transgene rescues the *ced-3(lf)* defect

Genotype	No. of cell corpses [a]	Range of corpses
ced-1(e1735)	31.2 ± 1.4	29~34
ced-1(e1735); ced-3(n717)	2.0 ± 1.3	0~4
ced-1(e1735) smIs10; ced-3(n717)	31.4 ± 2.4	27~36

[a] Cell corpses were scored at the 4-fold embryonic stages. Data shown are mean ± S.D. 20 embryos from each strain were scored.